KINETICS OF REDUCTION OF Cu IONS IN MFI ZEOLITE INVESTIGATED BY H_2-TPR METHOD

Roman BULÁNEK[1,*] and Pavel ČIČMANEC[2]

Department of Physical Chemistry, Faculty of Chemical Technology, University of Pardubice, nám. Čs. legií 565, 532 10 Pardubice, Czech Republic;
e-mail: [1] roman.bulanek@upce.cz, [2] pavel.cicmanec@upce.cz

Received May 13, 2008
Accepted August 18, 2008
Published online October 3, 2008

The temperature programmed reduction with hydrogen (H_2-TPR) profiles of the Cu-MFI zeolite matrix were measured. The effect of the Cu ions loading and the heating rate on the H_2-TPR profiles was investigated. The obtained TPR profiles were evaluated by different methods in order to obtain kinetic parameters and the reduction process mechanism. It was observed that the results given by convenient methods based on the simple power-law kinetics cannot be used for evaluation of at least the reduction of monovalent copper. Based on the reaction rate dependence on the degree of conversion, an autocatalytic reaction mechanism model was suggested for monovalent copper reduction. The autocatalytic effect was ascribed to nanoclusters of metallic copper, which is formed during the reduction. The parameters of this model were obtained by fitting the reaction rate equation to experimental data. The simulated TPR profiles well describe the position and relative height of peaks in experimental TPR profiles. Using our approach to evaluation of kinetic parameters we found the activation energies for reduction of Cu^{2+}, direct reduction of Cu^{+} and autocatalytic reduction of Cu^{+} equal to 91, 67 and 38 kJ mol^{-1}, respectively. All the mentioned processes are controlled by the kinetics of order ca. 1.5.

Keywords: Copper; Reduction; H_2-TPR; Zeolite; MFI; ZSM-5; Cu; Kinetics; Kissinger method; Iso-conversion Friedman method; Malek method.

The copper-exchanged high-silica zeolites attract great attention due their unique activity in various redox reaction and specific adsorption behavior. Cu-MFI zeolites are active in decomposition of NO_x [1], selective catalytic reduction of NO with hydrocarbons[2,3] and decomposition of N_2O [4], which can be a path of the abatement of the air pollutants. More recently these materials attract attention as a model system of metallic nanoclusters, which are formed during the reduction of Cu ions coordinated in zeolite matrices, and become a new generation of advanced catalytic materials[5,6]. Very recently, a new efficient π-complexation sorbents, such as Cu^{+} zeo-

Collect. Czech. Chem. Commun. 2008, Vol. 73, Nos. 8–9, pp. 1132–1148

doi:10.1135/cccc20081132

lites, have been developed for a number of applications in separation and purification such as separation of paraffin/olefin mixtures and purification of H_2 from CO [7,8]. Very often, Cu^+ act as active centers of both reactions and adsorption. Therefore, considerable attention is paid to elucidation of the structure, nature and redox behavior of Cu ions in these materials both experimental and theoretical approaches and their combination[9–28].

The temperature programmed reduction with hydrogen (H_2-TPR) is one of the most popular techniques for characterization of redox properties. The TPR was introduced by Jenkins[29] in the mid-seventies as a method of investigation of redox behavior of oxides. The method is based on monitoring changes in the redox state of the measured sample in hydrogen atmosphere as a function of the linearly increased temperature. The H_2-TPR is mostly used only as a technique for relative comparison of redox properties of a set of similar catalysts. Detailed information on mechanism and kinetic parameters of reduction can be indirectly determined by analysis of experimental TPR curves. Evaluation of TPR spectra is based on simplified assumptions and several methods were derived to obtain information on the activation energy or kinetics of reduction[20,30–32]. These methods were derived to describe reduction of oxide materials assuming simple power-law kinetics but their applicability is limited. Application of the approach to investigation of reduction of atomically dispersed metal ions in zeolites led to incorrect results. To the best of our knowledge, there are no publications on theoretical analysis, mathematical model and simulation of TPR spectra of Cu-zeolites in order to obtain kinetic parameters of reduction.

It is well known that H_2-TPR profiles of Cu-zeolites exhibit two dominant reduction peaks. The basic problem of interpretation of experimental H_2-TPR curves was to determine whether the Cu^{2+} ions coordinated at various sites of the zeolite matrix are directly reduced to metal copper or whether the reduction is a consecutive process via relatively stable species of monovalent copper. Quantitative studies of the reduction process on Cu-MOR [21,22], Cu-FAU [18–20,33] and Cu-MFI zeolites[11–14,34] described the reduction of Cu^{2+} ions by a two-step mechanism. Recently, a consecutive mechanism of the Cu reduction was proven by using combined H_2-TPR and in-situ EXAFS technique for reduction of Cu ions exchanged in the MFI zeolite[10,16,17]. At present, the two-step reduction process with Cu^+ as a stable intermediate is generally accepted. Nevertheless, if bulk CuO was present on the catalyst surface, a one-step two-electron reduction of Cu^{2+} to Cu^0 would be observed[11,14]. The situation in other types of zeolite or mesoporous materials is not necessarily the same, as it was observed in the

case of the MCM-48, where the direct one-step reduction of copper was proven[35,36].

Here we report kinetic analysis of the H_2-TPR pattern of Cu-MFI zeolites. Kinetic parameters of reduction of Cu^{2+} and Cu^{+} ions in Cu-MFI zeolites, resulting from methods using different power-law kinetic models and information on dependence of reaction rate on conversion, are compared and discussed.

EXPERIMENTAL

Na-form of zeolite of ZSM-5 (MFI) type with Si/Al ratio 14.1 was kindly provided by the Institute of Oil and Hydrocarbon Gases, Slovnaft, Slovakia. Cu ions were introduced into zeolite by the conventional wet ion exchange process. More details about condition of preparation and characterization of resulted materials are reported in ref.[11]. The zeolites are denoted as follows: CuNa-MFI-Cu/Al ratio.

Reduction of all prepared Cu-zeolites (calcined in a flow of oxygen (25 cm^3 min^{-1}) at 450 °C for 2 h prior to TPR and cooled in a flow of oxygen) was monitored at the heating rate (β) 10 °C min^{-1} in the range of 20–1000 °C. CuNa-MFI-0.44 sample was measured at the additional heating rates 4, 6, 8, 15 and 20 °C min^{-1}. A quartz laboratory-scale reactor was charged with 150 mg of zeolite. Changes in the concentration of the reduction gas containing 5 vol.% of H_2 in argon, with the total flow rate 25 cm^3 min^{-1}, were monitored simultaneously with a thermal conductivity detector (Regom Inst., Czech Republic) and quadrupole mass spectrometer OmniStar GDS 300 (Pfeiffer Vacuum, Austria). The consumption of hydrogen was calibrated using the CuO–MgO mixtures of known CuO contents (Fluka). All experimental data were fitted with sum Gaussian curves for the smoothing purpose. Two Gaussians were used to describe the shapes of TPR peaks.

THEORY

The evaluation of kinetic parameters of the reduction process used in this paper is briefly described in this section. It is possible to find several methods to calculate apparent activation energies that were derived for description of TPR profiles of oxide materials. The most frequently used method is the Kissinger method[37,38]. This method has been used in literature to determine the apparent activation energies of solid-state reactions from plots of the logarithm of the heating rate divided by squared temperature at the maximum reaction rate versus the reciprocal temperature at the maximum reaction rate in experiments with constant heating rate. The apparent activation energy can be determined by the Kissinger method without precise knowledge of the reaction mechanism, using the following equation:

$$2 \ln T_{max} - \ln \beta + p \ln [G] + (q - 1) \ln [S] = \frac{E_a}{RT} + \text{const.} \qquad (1)$$

where [G] and [S] denote the concentration of the reduction gas and the concentration of reduced species at temperature of the maximum of the TPR peak, respectively, p and q values are the kinetic orders of the reaction in gaseous and solid components in the reduction mixture, respectively, E_a value is the activation energy of the reaction, R is the gas constant (8.314 J K^{-1} mol^{-1}), T the thermodynamic temperature (in K) and β is the heating rate. The concentration of hydrogen is often substantially higher than that of the reduced species and, therefore, its concentration is usually treated as a constant.

This and the following two methods are based on modeling the H_2-TPR method using the power-law kinetic model[39]. The kinetic equation is expressed as:

$$r = \frac{\mathrm{d}X}{\mathrm{d}t} = k'(T)\,(1 - X)^q \qquad (2)$$

where X value is the conversion degree of the reduced species, q is the reaction order with respect to reduced species and k' is a rate constant. The rate constants are usually expressed as function of temperature using the Arrhenius equation:

$$k(T) = A \exp\left(-\frac{E_a}{RT}\right) \qquad (3)$$

where A is a pre-exponential factor (in Eq. (*2*) it has the dimension of time^{-1}) and E_a is the apparent activation energy (in J mol^{-1}).

Another approach to TPR pattern evaluation is isoconversion Friedman method[40,41]. This method can be used for estimation of the apparent activation energy as a function of the conversion degree without knowledge of the reaction order and mechanism. The method is applicable to a set of experimental TPR curves measured at different heating rates. Nevertheless, the applicability of this method is restricted to processes whose reduction rate can be expressed as the product of a temperature function and a second function of conversion. The apparent activation energy, E_a, at a specific degree of conversion is evaluated from the slope of the plots obtained from the equation (Eq. (*4*)) known in the literature as the isoconversional line.

$$\frac{\mathrm{d}X}{\mathrm{d}t} = k'(T)\,(1 - X)^q \Rightarrow \ln\left(\frac{\mathrm{d}X}{\mathrm{d}t}\right) = \ln(A\,f(X)) - \frac{E_a}{RT} \qquad (4)$$

Once the apparent activation energy has been determined, the kinetic model can be found that best describes the measured set of TPR data. It can be shown that it is useful for this purpose to define special function $y(X)$, which can easily be obtained by simple transformation of experimental data (Malek method)[42]. This function can be expressed as follows:

$$y(X) = \frac{\mathrm{d}X}{\mathrm{d}t} \exp\left(\frac{E_a}{RT}\right) \propto f(X) . \qquad (5)$$

Function $y(X)$ is proportional to the right-hand side of the kinetic equation and its normalized form can be used for determining the reaction order. If we assume that kinetics can be expressed by a simple power law, the reaction order can be determined from a plot of log $y(X)$ on the log $(1 - X)$ (Eq. (*6*)).

$$\ln(y(X)) = \text{const.} + q \ln(1 - X) \qquad (6)$$

If a simple power-law kinetic approach cannot be applied, the methods discussed above need not lead to reliable results with a physical meaning. In this case, the experimental data of the H_2-TPR profiles measured at different rates of the temperature growth allow to obtain information on the reduction kinetics using the dependence of the reaction rate on the conversion degree of reduced species at a certain temperature because different conversions are reached for various rates of temperature growth (β) at the different temperatures. This method was originally used for the description of reduction of oxide systems but it can be more useful for ion-exchanged zeolites. This is due to the fact that the kinetics of the reduction of isolated ions in the zeolite matrix is not complicated by mass and heat transport effects, which strongly affect the kinetics of the TPR of bulk oxides. The conversion degree as a function of temperature can be calculated as an integral of the TPR peak from zero to the desired temperature divided by the total area of the peak. The time derivative of the conversion was calculated as the height of the peaks divided by total area of the peak and multiplied by the rate of temperature growth (β).

All the mentioned methods possess intrinsic limitations and the results obtained by these methods should be treated very carefully and compared with the results of other methods.

RESULTS AND DISCUSSION

Experimental H_2-TPR Profiles

Figure 1 presents the TPR curves of all investigated Cu-MFI materials. The two separated peaks are perceptible in all TPR profiles except for sample with the highest Cu loading where the third sharp peak at the 250 °C can be observed (Fig. 1, curve e). A sharp peak appearing at high-temperature side of the first major reduction peak in the H_2-TPR pattern of Cu-MFI zeolites was attributed to Cu^{2+} in dispersed undefined CuO species, reduced in a one-step process directly to Cu^0 in agreement with refs[11,14]. This assignment corresponds also to the H_2-TPR curve of CuO on silica, where the reduction peak occurred at the same temperature (see the inset in Fig. 1). The amount of Cu^{2+} in cationic sites in this sample was obtained as total amount of Cu diminished by value corresponds to amount of CuO for this sample in the following data processing. The position of the low-temperature peak changes only slightly in the range 218–232 °C in contrasts to that of the high-temperature peak in the range 340–580 °C. The temperature of the peak maximum increases with decreasing Cu loading in the zeolite matrix.

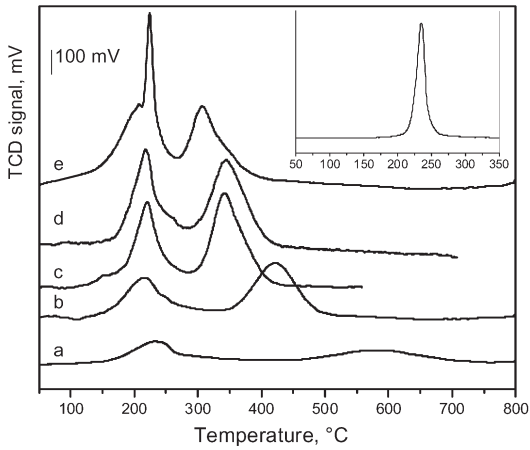

FIG. 1
The H_2-TPR profiles for MFI zeolites with different Cu loading. Curve: CuNa-MFI-0.19 (a), CuNa-MFI-0.37 (b), CuNa-MFI-0.44 (c), CuNa-MFI-0.52 (d), CuNa-MFI-0.59 (e). Inset: H_2-TPR profile of CuO supported on amorphous silica

In order to determine the apparent activation energy by the Kissinger methods, we measured six TPR spectra of zeolite CuNa-MFI-0.44. The individual experiments only differed in the rate of temperature increase in the reactor, ranging from 4 to 20 °C per minute. The dependence of the TPR profiles for CuNa-MFI-0.44 on temperature growth (β) is shown in Fig. 2. The character of the TPR profiles is the same for all measurements. Also two separated TPR peaks of approximately the same heights are present. The increase in the β parameter causes shifts of the maxima of both the peaks towards higher temperatures, the shifts being more pronounced for the high-temperature peaks.

The total consumption of hydrogen was determined; it was observed that the H_2/Cu ratio is close to unity in all cases (H_2/Cu = 0.98 ± 0.02), which means that complete reduction of the exchanged Cu^{2+} to metallic copper occurred. The investigation of the reduction of Cu ions in the MFI matrix[10,16,17] by the EXAFS technique proved that the reduction of copper in the zeolite matrix is a consecutive process where the reduction of Cu^{2+} to Cu^{+} starts at 200 °C. The Cu^{+} ions are stabilized by the zeolite matrix and their reduction starts after nearly complete reduction of the divalent copper. This fact is supported by the fact that the areas of both the low-temperature and the high-temperature peaks are approximately the same[11]. In addition, the peaks are nearly separated (the overlap is less than 5%), which

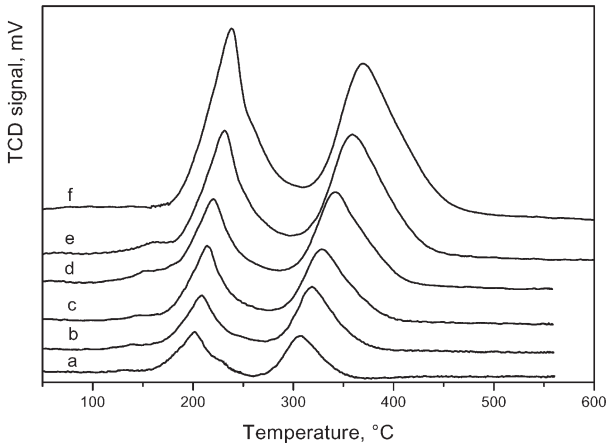

FIG. 2
The H_2-TPR profiles of the CuNa-MFI-0.44 zeolite using various heating rates (in °C min^{-1}): 4 (a), 6 (b), 8 (c), 10 (d), 15 (e), 20 (f)

implies that the Cu^{+} reduction starts after almost complete reduction of Cu^{2+}. Based on this information we can attribute the first (low-temperature) peak of the TPR profiles to reduction of divalent copper and the high-temperature peak to reduction of monovalent copper.

In the following text, the results of theoretical evaluation of the above-described experimental data are reported and discussed with the aim to obtain information on the mechanism of Cu ion reduction as well as the kinetic parameters.

Estimation of Kinetic Parameters of Cu Ions Reduction

Figure 3 presents the dependence of logarithm of the β/T_{max}^2 ratio on the reciprocal temperature of the TPR peak maximum according to the Kissinger method (see Experimental). The values of the activation energy, obtained from the slopes of the data plotted in Fig. 3, were 80 and 65 kJ mol^{-1} for the reduction of Cu^{2+} and Cu^{+}, respectively. Similar values of the apparent activation energies of reduction of Cu ions in the FAU zeolite matrix (84 and 64 kJ mol^{-1}) were published by Hurst et al.[30,31] using this method. One of the values of apparent activation energy is close to the value published for that of bulk CuO (67 ± 10 kJ mol^{-1})[30].

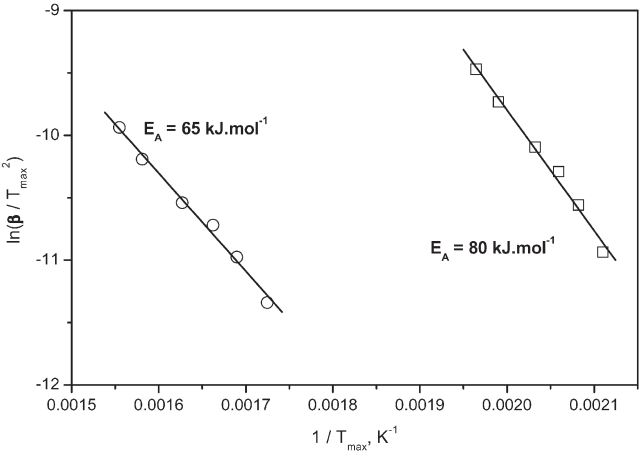

FIG. 3
The dependence of ln (β/T_{max}^2) on the reciprocal temperature of the peak maxima: □ experimental points, the solid line is a linear fit for the low-temperature peak; ○ experimental points, the solid line is a linear fit for the high-temperature peak

The H_2-TPR profiles of Cu ion-exchanged in the MFI cannot be described by the method based on the power-law approach because the shifts of the high-temperature peaks are more pronounced than those of the low-temperature peaks. This is clear evidence of the fact that reduction of monovalent copper is the process with lower activation energy than reduction of divalent copper. This also means that if the process occurred at higher temperature than reduction of Cu^{2+} ions, the rate constant expressed as the Arrhenius equation (Eq. (*3*)) should have a substantially lower value of the pre-exponential factor *A*. On the other hand, the lowering of the pre-exponential factor causes broadening and decreasing of the TPR peaks, which was not observed in experimental data. The high-temperature peaks in Figs 1 and 2 have approximately the same heights as the low-temperature peaks as mentioned above. This means that the mechanism of Cu^{+} reduction is more complex and it is necessary to describe the process by a more complex kinetic model.

Prior to detailed investigation of Cu^{+} reduction, its kinetics was investigated by Friedman and Malek methods with the aim to validate the results obtained by the Kissinger method. The apparent activation energies resulting from Friedman isoconversion method in dependence on the Cu^{2+} conversion degree are shown in Fig. 4. It is clearly seen that the obtained activation energies are nearly constant in a wide range of conversion de-

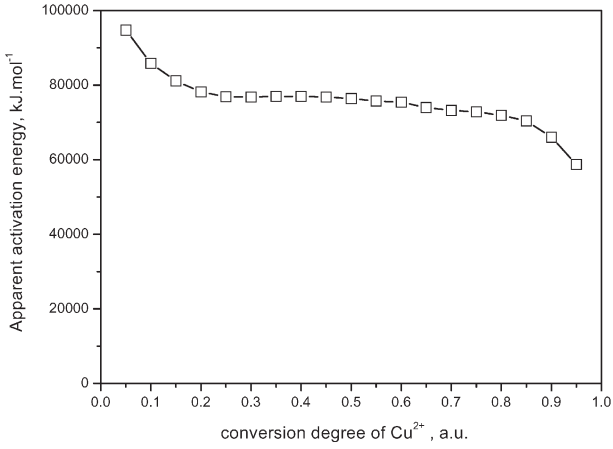

FIG. 4
The dependence of apparent activation energies for reduction of Cu^{2+} ions, obtained by the Friedman method, on the conversion degree

grees from 0.15 to 0.85. The activation energy in this region is 75 kJ mol^{-1}, which is close to the value obtained by Kissinger method (80 kJ mol^{-1}). The deviation of the activation energies at the lowest and highest degrees of conversion are probably caused by uncertainties associated with subtraction of baseline or by a low signal-to-noise ratio at the start and end of the peak. The fact that the activation energy is constant over a wide range of conversions indicates the possibility of describing the reduction process reflected in the low-temperate peak, by a simple kinetic model based on the power law.

The data from Friedman plot do not provide any information about the reaction order of the investigated reduction process. For this purpose, Malek method was used to estimate the shape of the reaction rate dependence on the Cu^{2+} conversion and the most proper reaction order. The dependence of log $y(X)$ defined by Eq. (5) on the log $(1 - X)$ for the TPR pattern of CuNa-MFI-0.44 sample with different heating rates is presented in Fig. 5. The slope of the dependence is equal to the kinetic order of the reaction. The values obtained from this plot ranged from 1.18 to 1.60, with the average value 1.43. This fractional reaction order is close to 1.5; such value can be explained by a dissociation mechanism taking place in the reaction. We assume that copper is reduced with hydrogen atoms which are produced after adsorption of gaseous hydrogen. Only some of the adsorption

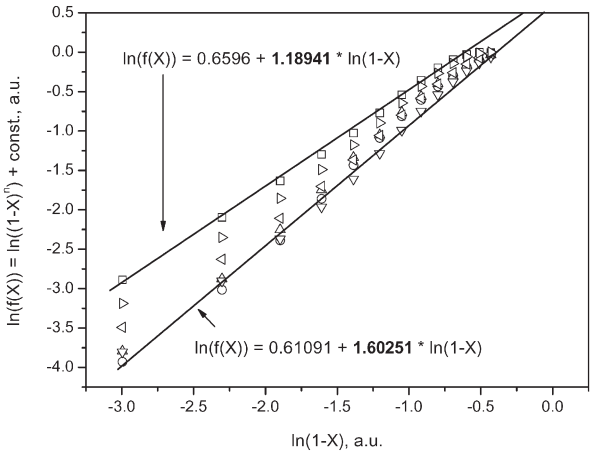

FIG. 5
The dependence of logarithm of Malek function $y(X)$ on logarithm $(1 - X)$. Slopes varying from 1.19 to 1.60. Various heating rates used (in °C min^{-1}): □ 4, ○ 6, △ 8, ▽ 10, ◁ 15, ▷ 20

sites can participate in the reduction of copper due to fast recombination of the hydrogen atoms and hence their concentration could be taken as proportional to the concentration of unreduced Cu^{2+} ions. If we express hydrogen adsorption by Henry law adsorption isotherm, we can write:

$$r_{red} = -\frac{d[Cu^{2+}]}{dt} = k_1[Cu^{2+}][H^{\bullet}] = k_1[Cu^{2+}]\sqrt{L K_{ads} p_{H_2}} = \\ = k_1[Cu^{2+}]\sqrt{[Cu^{2+}] K p_{H_2}} = k_1'[Cu^{2+}]^{1.5} \quad (7)$$

where r_{red} is the rate of reduction, k_1 the intrinsic rate constant of reduction, $[Cu^{2+}]$ concentration of Cu^{2+} ions, $[H^{\bullet}]$ concentration of hydrogen radicals, L overall concentration of adsorption sites, K equilibrium constant of adsorption and dissociation of hydrogen, p_{H_2} is partial pressure of hydrogen in gas, k_1' is the apparent rate constant. This means that the rate of reduction is proportional to concentration of Cu^{2+} ions raised to 3/2.

The presented results proved that the activation energy obtained by Kissinger method is valid and process is controlled by simple power-law based kinetics described by the order of 3/2. The application of Kissinger method to the high-temperature peak led to an unreliable value due to the above discussed discrepancy of the shape of TPR peaks and the low value of activation energy. Therefore, the reduction process manifesting itself in a high-temperature peak should be a more complex process which cannot be evaluated by the discussed isoconversion methods (Friedman and Malek methods).

The experimental data of the H_2-TPR profiles measured at different rates of temperature growths allows to obtain information about the kinetics of the reduction using the isothermal dependence of the reaction rate on the degree of conversion of reduced species, because the different conversion values are achieved for various heating rates (β) at a certain temperature. This method was originally used for the description of reduction of oxides but it can be more useful for ion-exchanged zeolites. This is due to the fact that the kinetics of the reduction of isolated ions in the zeolite matrix is not complicated by mass and heat transport effects, which strongly affect the kinetics of TPR of the bulk oxides. The conversion degree as a function of temperature was calculated by integration of the TPR peak from zero to the desired temperature divided by the total peak area. The time derivative

of the conversion was calculated as the height of the peaks divided by the total peak area and multiplied by the rate of temperature growth (β).

Figure 6 presents the dependences of the reaction rate on the conversion for the low-temperature peak at 210 and 230 °C. The power-law kinetic equation (Eq. (*2*)) was used to obtain values of both the activation energy and reaction order α by fitting experimental data to this equation. The activation energy and reaction order were 91 kJ mol^{-1} and ca. 1.5 ± 0.1, respectively. This value is in agreement with the result obtained by Malek method, indicating the reaction mechanism where the hydrogen dissociation plays the role of the rate-determining step.

The evaluation of the high-temperature peak was performed by the same method as in the case of the low-temperature peak. The points connected with dashed lines in Fig. 7 represent experimental dependence of the rate of reduction of monovalent copper on the degree of the conversion at temperatures from 290 to 390 °C. The dependences exhibit maxima for some temperatures, which is a typical feature of autocatalytic character of the reduction. It was previously observed[10,16,17] using the EXAFS technique that monovalent copper ions form clusters of metallic copper during reduction. The clusters reach diameters which are close to the diameters of the zeolite channels during the reduction[5,6,10,16,17]. It is well known that zeolite matrix stabilizes monovalent copper. The energy of reduction of Cu^{+} ions to

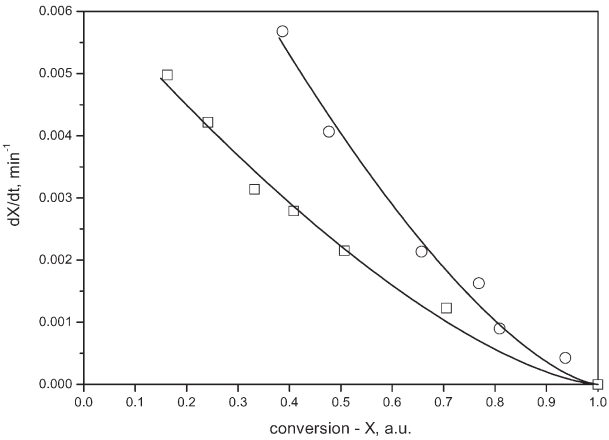

FIG. 6
The dependence of the reduction reaction rates on the degree of conversion for the low-temperature peak (in °C): □ 210, ○ 230; —— fitted values

monoatomic copper is ca. 280 kJ mol^{-1} based on quantum chemistry data[27]. Due to endothermic character of this reaction it can be expected that the activation energy of the reaction is even higher. Because the observed values of activation energy are substantially lower, it is necessary to expect that copper is not reduced to monoatomic copper. Based on this finding it is assumed that mobile clusters of metallic copper can play the role of the catalyst that increases the reduction rate of monovalent copper.

Based on these assumptions, the rate equation was suggested as follows:

$$r = \frac{\mathrm{d}X}{\mathrm{d}t} = k'_{\mathrm{start}}(T)\,(1-X)^{q_1} + k'_{\mathrm{ac}}(T)\,(1-X)^{q_2}\,X\,. \qquad (8)$$

It is the sum of two terms. The first is attributed to a slow "starting" reaction and the second to a fast autocatalytic step. The parameters of these equations were obtained by fitting the calculated dependences of the reaction rate on the conversion with shared kinetic parameters for all fitted curves. The calculated values of reaction rates are the solid lines presented in Fig. 7. The activation energy of the starting step was 67 kJ mol^{-1} and that of the autocatalytic step 38 kJ mol^{-1}. The reaction orders were also fitted. The orders of both reactions were approximately 1.5 as in the case of the

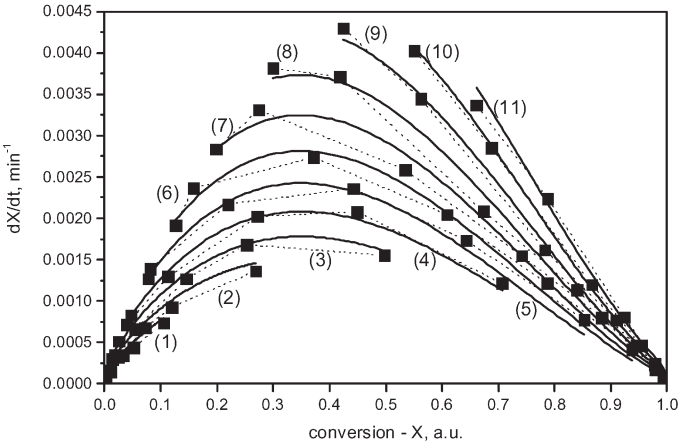

FIG. 7

The dependence of the reduction reaction rates on the degree of conversion for the high-temperature peak (in °C): 290 (1), 300 (2), 310 (3), 320 (4), 330 (5), 340 (6), 350 (7), 360 (8), 370 (9), 380 (10), 390 (11); ■ experimental values, —— fitted values

low-temperature peak. The assumed mechanism that can be attributed to such value was discussed above.

The simulated TPR profile was calculated on the basis of the information obtained on the kinetics of the Cu ion reduction in the MFI zeolite. Figure 8 presents a comparison of the experimental and simulated TPR profiles for the all TPR patterns of CuNa-MFI-0.44 with different heating rates. It is clearly seen that the simulated profile fits well the experimental data especially for the high-temperature peak. The experimental data for the low-temperature peak are rather higher than those for the simulated one. This effect can be caused by a small shoulder at the onset of the low-temperature peak, which affects the calculation of conversion and kinetic parameters. Nevertheless, the positions of peaks were correctly predicted by the model.

In the light of the proposed kinetic model for reduction of copper in MFI zeolites, we can explain the dramatic shift of the maxima of high-temperature reduction peaks of samples differing in the copper content (Fig. 1). The shift of the high-temperature reduction peak to lower temperatures with increasing copper content can be ascribed to faster formation of metallic cluster and a shorter distance between two neighboring copper ions or copper ion and the formed copper cluster. The higher the copper loading the shorter is the average distance between two copper species. In addition, the proposal is supported by changes in the shape and skew of the high-

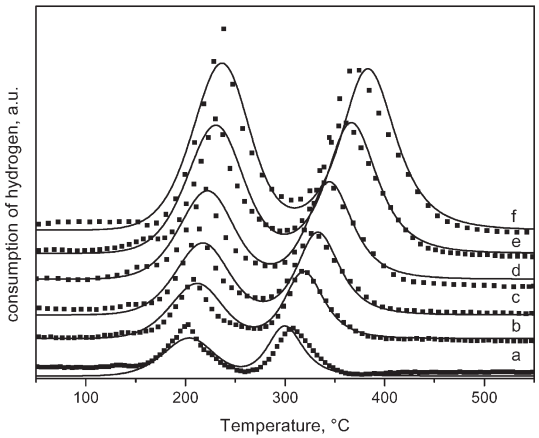

FIG. 8

The experimental (■) and calculated (——) H_2-TPR profiles of the CuNa-MFI-0.44 zeolite using various heating rates (in °C min^{-1}): 4 (a), 6 (b), 8 (c), 10 (d), 15 (e), 20 (f)

temperature peak of the TPR pattern of samples with different copper contents (see Fig. 1). The higher the copper content the more asymmetric is the peak. The tailing to higher temperature can be ascribed to longer distances to which copper clusters are transported at high conversions.

CONCLUSIONS

Based on the results of temperature-programmed reduction of Cu^{2+} ions exchanged in the MFI zeolite matrix we can conclude:

1) The application of conventional methods to the TPR profiles gives non-consistent results at least for reduction of monovalent copper. The activation energies can be used only as qualitative information about the changes in the TPR peak positions.

2) The reduction of monovalent copper is an autocatalytic process where the nanoclusters of metallic copper significantly enhance the rate of reduction of monovalent copper.

3) Using our approach to evaluation of kinetic parameters we found the activation energies for reduction of Cu^{2+}, direct reduction of Cu^{+} and autocatalytic reduction of Cu^{+} equal to 91, 67 and 38 kJ mol^{-1}, respectively. All the three processes are controlled by kinetics of a reaction order of 1.5.

4) The fractional value of reaction order of the reduction processes can be explained by a dissociation mechanism of the reaction.

SYMBOLS

A	frequency factor, definition-dependent
E_a	activation energy, J mol^{-1}
$f(X)$	general function of the conversion degree
k, k_1, k', k'_1, k'_{start}, k'_{ac}	rate constants, definition-dependent
K_{ads}, K'	equilibrium constants
L	surface concentration of adsorption sites, mol m^{-2}
p	reaction order of the gas reduction
p_{H_2}	relative partial pressure of hydrogen
q, q_1, q_2	reaction orders of the reduction of solid
r, r_{red}	time change of the conversion degree, s^{-1}
R	gas constant, 8.314 J K^{-1} mol^{-1}
t	time, s
T	thermodynamic temperature, K
T_{max}	temperature at the maximum of TPR peak, K
X	conversion degree
y	Malek function = $dX/dt \exp(E_a/RT)$, s^{-1}
β	heating rate, K s^{-1}
TPR	temperature-programmed reduction

MOR, MFI, FAU zeolite framework type codes set up by an UIPAC Commission on Zeolite Nomenclature
ZSM-5 trivial designation of MFI zeolite structure type
EXAFS extended X-ray absorption fine structure

Financial support of the Ministry of Education, Youth and Sports of the Czech Republic under projects LC512 and MSM0021627501 is highly acknowledged.

REFERENCES

1. Iwamoto M., Furukawa H., Mine Y., Uemura F., Mikuriya S., Kagawa S.: *J. Chem. Soc., Chem. Commun.* **1986**, 1272.
2. Iwamoto M., Yahiro H.: *Catal. Today* **1994**, *22*, 5.
3. Iwamoto M., Mizuno N., Yahiro H., Taylor K. C., Blanco J., Nam I. S., Bartholomew C. H., Metcalfe I. S., Iglesia E., Sinev M., Duprez D., Armor J., Misono M.: *Stud. Surf. Sci. Catal.* **1993**, *75*, 1285.
4. Li Y. J., Armor J. N.: *Appl. Catal., B* **1992**, *1*, L21.
5. Petranovskii V., Gurin V., Machorro R.: *Catal. Today* **2005**, *107–108*, 892.
6. Gurin V. S., Petranovskii V. P.: *Stud. Surf. Sci. Catal.* **2004**, *154*, 1661.
7. Sircar S.: *Ind. Eng. Chem. Res.* **2006**, *45*, 5435.
8. Huang H. Y., Padin J., Yang R. T.: *Ind. Eng. Chem. Res.* **1999**, *38*, 2720.
9. Bulánek R.: *Phys. Chem. Chem. Phys.* **2004**, *6*, 4208.
10. Neylon M. K., Marshall C. L., Kropf A. J.: *J. Am. Chem. Soc.* **2002**, *124*, 5457.
11. Bulánek R., Wichterlová B., Sobalík Z., Tichý J.: *Appl. Catal., B* **2001**, *31*, 13.
12. Beutel T., Sarkany J., Lei G. D., Yan J. Y., Sachtler W. M. H.: *J. Phys. Chem.* **1996**, *100*, 845.
13. Sarkany J., Sachtler W. M. H.: *Zeolites* **1994**, *14*, 7.
14. Sarkany J., Ditri J. L., Sachtler W. M. H.: *Catal. Lett.* **1992**, *16*, 241.
15. Palomino G. T., Fisicaro P., Bordiga S., Zecchina A., Giamello E., Lamberti C.: *J. Phys. Chem. B* **2000**, *104*, 4064.
16 Yamaguchi A., Inada Y., Shido T., Asakura K., Nomura M., Iwasawa Y.: *J. Synchrotron Radiat.* **2001**, *8*, 654.
17. Yamaguchi A., Shido T., Inada Y., Kogure T., Asakura K., Nomura M., Iwasawa Y.: *Bull. Chem. Soc. Jpn.* **2001**, *74*, 801.
18. Jacobs P. A., Tielen M., Linart J. P., Uytterhoeven J. B., Beyer H.: *J. Chem. Soc., Faraday Trans. 1* **1976**, *72*, 2793.
19. Jacobs P. A., Wilde W. D., Schoonheydt R. A., Uytterhoeven J. B., Beyer H.: *J. Chem. Soc., Faraday Trans. 1* **1976**, *72*, 1221.
20. Herman R. G., Lunsford J. H., Beyer H., Jacobs P. A., Uytterhoeven J. B.: *J. Phys. Chem.* **1975**, *79*, 2388.
21. Torre-Abreu C., Henriques C., Ribeiro F. R., Delahay G., Ribeiro M. F.: *Catal. Today* **1999**, *54*, 407.
22. Torre-Abreu C., Ribeiro M. E., Henriques C., Delahay G.: *Appl. Catal., B* **1997**, *14*, 261.
23. Bludský O., Nachtigall P., Čičmanec P., Knotek P., Bulánek R.: *Catal. Today* **2005**, *100*, 385.

24. Bludský O., Šilhan M., Nachtigall P., Bucko T., Benco L., Hafner J.: *J. Phys. Chem. B* **2005**, *109*, 9631.
25. Bulánek R., Čičmanec P., Knotek P., Nachtigallová D., Nachtigall P.: *Phys. Chem. Chem. Phys.* **2004**, *6*, 2003.
26. Davidová M., Nachtigallová D., Bulánek R., Nachtigall P.: *J. Phys. Chem. B* **2003**, *107*, 2327.
27. Nachtigallová D., Nachtigall P., Sauer J.: *Phys. Chem. Chem. Phys.* **2001**, *3*, 1552.
28. Nachtigallová D., Nachtigall P., Sierka M., Sauer J.: *Phys. Chem. Chem. Phys.* **1999**, *1*, 2019.
29. Jenkins J. W., McNicol B. D., Robertson S. D.: *Chemtech* **1977**, *7*, 316.
30. Hurst N. W., Gentry S. J., Jones A., McNicol B. D.: *Catal. Rev.–Sci. Eng.* **1982**, *24*, 233.
31. Gentry S. J., Hurst N. W., Jones A.: *J. Chem. Soc., Faraday Trans. 1* **1979**, *75*, 1688.
32. Falconer J. L., Schwarz J. A.: *Catal. Rev.–Sci. Eng.* **1983**, *25*, 141.
33. Beyer H., Jacobs P. A., Uytterhoeven J. B.: *J. Chem. Soc., Faraday Trans. 1* **1976**, *72*, 674.
34. Sarkany J., Sachtler W. M. H.: *Stud. Surf. Sci. Catal.* **1995**, *94*, 649.
35. Tkachenko O. P., Klementiev K. V., van den Berg M. W. E., Koc N., Bandyopadhyay M., Birkner A., Woll C., Gies H., Grunert W.: *J. Phys. Chem. B* **2005**, *109*, 20979.
36. Tkachenko O. P., Klementiev K. V., Koc N., Yu X., Bandyopadhyay M., Grabowski S., Gies H., Grunert W.: *Stud. Surf. Sci. Catal.* **2004**, *154*, 1670.
37. Kissinger H. E.: *Anal. Chem.* **1957**, *29*, 1702.
38. Kissinger H. E.: *J. Res. Natl. Bur. Stand.* **1956**, *57*, 217.
39. Cioci F., Lavecchia R., Fierro G., LoJacono M., Inversi M.: *Thermochim. Acta* **1996**, *287*, 351.
40. Friedman H. L.: *J. Polym. Sci., Part C: Polym. Symp.* **1964**, 183.
41. Friedman H. L.: *J. Polym. Sci.* **1960**, *45*, 119.
42. Málek J.: *Thermochim. Acta* **1992**, *200*, 257.